

January 10, 2011

Higgsino dark matter model consistent with galactic cosmic ray data and possibility of discovery at LHC-7

Ning Chen
Stony Brook University

Daniel Feldman
University of Michigan

Zuowei Liu
Stony Brook University

Pran Nath
Northeastern University

Gregory Peim
Northeastern University

Recommended Citation

Chen, Ning; Feldman, Daniel; Liu, Zuowei; Nath, Pran; and Peim, Gregory, "Higgsino dark matter model consistent with galactic cosmic ray data and possibility of discovery at LHC-7" (2011). *Physics Faculty Publications*. Paper 452. <http://hdl.handle.net/2047/d20004229>

Higgsino dark matter model consistent with galactic cosmic ray data and possibility of discovery at LHC-7

Ning Chen,¹ Daniel Feldman,² Zuowei Liu,¹ Pran Nath,³ and Gregory Peim³

¹*C.N. Yang Institute for Theoretical Physics, Stony Brook University, Stony Brook, New York 11794, USA*

²*Michigan Center for Theoretical Physics, University of Michigan, Ann Arbor, Michigan 48109, USA*

³*Department of Physics, Northeastern University, Boston, Massachusetts 02115, USA*

(Received 5 October 2010; published 10 January 2011)

A solution to the PAMELA positron excess with Higgsino dark matter within extended supergravity grand unified (SUGRA) models is proposed. The models are compliant with the photon constraints recently set by Fermi-LAT and produce positron as well as antiproton fluxes consistent with the PAMELA experiment. The SUGRA models considered have an extended hidden sector with extra degrees of freedom which allow for a satisfaction of relic density consistent with WMAP. The Higgsino models are also consistent with the CDMS-II and XENON100 data and are discoverable at LHC-7 with 1 fb^{-1} of luminosity. The models are testable on several fronts.

DOI: 10.1103/PhysRevD.83.023506

PACS numbers: 95.35.+d, 12.60.Jv, 13.85.Rm, 98.70.Sa

I. INTRODUCTION

Recently, experiments detecting galactic cosmic rays have begun to probe the nature of the dark matter in the halo. The large excess observed of high energy positrons in the PAMELA experiment [1] and the null results in the search for gamma ray lines with the Fermi-LAT experiment [2] present a challenge for particle theory. Some particle physics explanations have been proposed to explain the PAMELA data consistent with the relic abundance of dark matter including: a Breit-Wigner enhancement [3], a non-perturbative Sommerfeld enhancement [4,5], and other possibilities [6–10]. A nonthermal cosmological history is also a solution [11–13]. Several astrophysics explanations have also been sought [14]. Within supersymmetry the positron excess can arise from the annihilation of neutralinos [lightest supersymmetric particle (LSP)] into W^+W^- and/or ZZ . This comes about when the LSP is a pure wino [11,13], a mixed wino-bino [6,15], or a Higgsino [16–19]. However, a wino LSP produces a large amount of monochromatic photons in its annihilation products which is edging close to the current upper limit set by the Fermi-LAT data [15].

Here we present a supersymmetric model, which in contrast to other proposed models, has mostly a Higgsino LSP and can explain the relic abundance of dark matter. In addition, we show that such a model fits the positron excess from PAMELA [1] and is consistent with the antiproton flux, as well as with data from monochromatic photons that arise via loop diagrams in the neutralino annihilation processes $\chi\chi \rightarrow \gamma\gamma, \gamma Z$ [20]. We note that a bino-like LSP can also explain the PAMELA positron data when a substantial size boost factor from the halo is allowed [21].

The monochromatic photon constraints from FERMI become very relevant when one tries to fit the PAMELA positron data via dark matter annihilations in the galactic halo, as the cross section needed to explain such data is

much larger than the naive estimation of the dark matter annihilation cross section from a thermal history. This expectation for the relic abundance, however, can be modified which will be discussed. Such a modification can open new parameter space in SUSY models where the relic density of dark matter is consistent with observations and the flux of cosmics from dark matter at present temperatures can account for the data. This has implications for signatures of supersymmetry at the Large Hadron Collider in the frameworks we discuss below.

II. EXTENDED ABELIAN MODELS AND ENHANCEMENT OF RELIC ABUNDANCE

The simplest extension of the standard model (SM) which is gauge invariant, renormalizable, and unitary arises through a Stueckelberg mechanism [22,23]. A $U(1)$ gauge boson V_μ gains mass M through a Stueckelberg mechanism [24] by directly absorbing an axion field σ through the combination $(MV_\mu + \partial_\mu\sigma)^2$ which is gauge invariant under the transformation $\delta V_\mu = \partial_\mu\lambda, \delta\sigma = -M\lambda$, and thus a transition to the unitary gauge produces a massive vector gauge boson without the necessity of a Higgs mechanism. It is also well known that the Stueckelberg mechanism arises quite naturally from a Green-Schwarz mechanism [25] with appropriate transformations. Further, in reduction of higher dimensional theories the masses of the Kaluza-Klein states arise from a Stueckelberg mechanism and not from a Higgs mechanism. The Stueckelberg mechanism is indeed quite generic in string theories (see e.g. [26]), in extended supergravity theories, and in the compactification of higher dimensional theories (for a review, see [27]).

Interesting new physics arises if there is a hidden sector with minimally a $U(1)$ gauge field that mixes with the hypercharge of the SM sector. A supersymmetric generalization of the Stueckelberg mechanism leads to an extended neutralino sector, i.e., where for each extra $U(1)$

factor one has two extra Majorana fields (Stinos) which mix with the minimal supersymmetric standard model (MSSM) neutralinos. The above considerations generalize to a set of Abelian $U(1)_X^n$ gauge groups, and such extensions lead to a mixing between fields in each sector via gauge kinetic energy mixings and mass mixings.

We implement this extension to study a class of supergravity unified models which allow the possibility of explaining the PAMELA data without recourse to large clump factors in the halo of the Galaxy. We uncover a new situation where the LSP is actually a nearly pure Higgsino under radiative electroweak symmetry breaking with mass in the range $\sim(110\text{--}190)$ GeV with the hidden sector components of the LSP being suppressed.

Thus we consider a supergravity grand unified model [28,29] having an extra hidden sector with a product gauge group $U(1)_X^n$ [6] which mixes with the hypercharge via mass terms generated by the Stueckelberg mechanism and without loss of generality via gauge kinetic mixing. For simplicity, we give a summary for the case of a single $U(1)_X$, and the generalization for a product gauge group follows analogously. In the vector sector the mass mixing and gauge kinetic mixing is of the form $-2M_X M_Y X^\mu Y_\mu - (\delta/2)X^{\mu\nu}Y_{\mu\nu}$, and in the neutralino sector the mass mixing is of the form $\psi_{\text{st}}(M_X \lambda_X + M_Y \lambda_Y) + \text{h.c.}$ while the kinetic mixing leads to $-i\delta(\lambda_X \sigma \cdot \partial \bar{\lambda}_Y + (Y \leftrightarrow X))$, where X denotes the hidden sector $U(1)$ and Y is the hypercharge of the MSSM; ψ_{st} is a fermionic field that arises out of a chiral Stueckelberg supermultiplet and $M_Y : M_X$ and δ are small, i.e. on the order of 10^{-2} or smaller [23]. Such additional states remain in contact with the thermal bath prior to freeze-out in the early universe. In the absence of hidden sector soft masses, a direct study of the mass matrix in the neutralino sector gives rise to a mass degeneracy g_{hid} for the hidden sector neutralinos with the LSP, which in turn, can have a degeneracy g_{vis} with other visible sector sparticles [30]. Coannihilations can then produce an enhancement of the relic density by a factor f_E [6] so that

$$\Omega_{\tilde{\chi}^0} h^2 \simeq f_E \times \Omega_{\tilde{\chi}^0}^{\text{MSSM}} h^2, \quad f_E = \left[1 + \frac{g_{\text{hid}}}{g_{\text{vis}}} \right]^2. \quad (1)$$

Generalizing to the case of a $U(1)_X^n$ extended hidden sector $g_{\text{hid}} = 2n$, and thus for the case $g_{\text{vis}} = 1$, one finds $f_E = (2n + 1)^2$ which gives $f_E = 25(49)$ for $n = 2(3)$. In this extended model the neutralino mass matrix will be $(4 + 2n) \times (4 + 2n)$ dimensional. We assume that the LSP lies in the visible (MSSM) sector. Because of coannihilations in the visible sector, the full enhancement is never achieved, however one finds large enhancements of size (10–20) or larger with a degenerate hidden sector and only 2–3 additional $U(1)$ s which is sufficient for compatibility with the WMAP constraint [31] since the models considered have the relic density in the range $\sim(2\text{--}6) \times 10^{-3}$ if there was no Abelian hidden sector.

III. LOW MASS HIGGSINO LSP IN EXTENDED SUGRA AND FERMI PHOTONS

We discuss now the details of the Higgsino-like neutralino models. Since the extra weak mixing discussed above is small, it has negligible effects on the soft parameters at the weak scale. The model parameters that dictate annihilation cross sections can then be described by the input parameters given in Table I. The models P1–P3 listed in Table I have a neutralino that is dominantly a Higgsino, with about 2% remaining in the gaugino content. For comparison, we also exhibit the mixed wino-bino (WB) model [6] which has a significant wino content $\sim 49\%$ of the total eigencontent along with a comparable bino content. All four models satisfy the current experimental constraints from flavor physics and limits on sparticle masses (see e.g. [33]). Their neutralino masses lie in the range (110–190) GeV and have a spin independent cross section of size $(5\text{--}10) \times 10^{-45}$ cm² consistent with the upper bounds from the CDMS-II and XENON100 [34]. Further, some of the models possess several rather light sparticles in their spectra, namely, the charginos, neutralinos, gluino and in some cases the stop, and are thus good candidates for discovery at the LHC.

In Table II we give the theoretical predictions of the Higgsino LSP models for the γZ and $\gamma\gamma$ modes and exhibit the current upper limits from the Fermi-LAT search for photon lines using three different halo profiles. One finds that the theoretical predictions for the Higgsino models (P1–P3), are well below the current upper bounds from Fermi-LAT, by about a factor of 10, for the most restrictive profile, while the mixed wino-bino model, WB, is close to the edge of the limits. There are sources of photons arising from bremsstrahlung that could mimic the line signature of monochromatic photons. The contributions from bremsstrahlung to the line signals can be significant or even dominant over the ones from the loop processes [35]. However, the additive effects from bremsstrahlung to the line source are small for the models considered here which

TABLE I. Parameters which produce an LSP which are mostly Higgsino (P1–P3), or mixed WB. Here $m_0(A_0)$ is the universal scalar mass (trilinear coupling), M_1, M_2, M_3 are the gaugino masses at the GUT scale for the gauge groups $U(1)_Y, SU(2)_L, SU(3)_C$, and $\tan\beta$ is the ratio of the two Higgs vacuum expectation values in the MSSM. The parameters that enter the neutralino mass matrix at scale $Q = \sqrt{M_{\tilde{t}_1} M_{\tilde{t}_2}}$ are (μ', M'_1, M'_2, M'_3) , where μ' is the Higgs mixing parameter. The models have also been run through both SUSPECT and SOFTSUSY via MICROMEAS [32]. Here $m_{\text{top}}^{\text{pole}} = 173.1$ GeV.

Model	m_0	M_1	M_2	M_3	A_0	$\tan\beta$	μ'	M'_1	M'_2	M'_3
P1	1033	1600	1051	120	2058	13	195	683	836	259
P2	1150	1600	1080	160	2080	15	152	684	859	347
P3	950	1425	1820	748	1925	25	109	617	1453	1589
WB	2000	400	210	200	300	5	562	170	163	441

TABLE II. Cross sections $\langle\sigma v\rangle_{\gamma Z}$ and $\langle\sigma v\rangle_{\gamma\gamma}$ upper limits (10^{-27} cm³/s) [2] for 3 halo profiles [Einasto, Navarro-Frenk-White (NFW), Isothermal], along with predictions for (P1–P3) and WB. The mostly Higgsino models (P1–P3) are unconstrained by any profile while the mixed wino-bino model, WB, is on the edge.

E_γ	Einasto	NFW	Isothermal	Model	$\langle\sigma v\rangle_{\gamma Z, [\gamma\gamma]}^{\text{theory}}$
180[190]	4.4[2.3]	6.1[3.2]	10.4[5.5]	P1	0.24[0.08]
130[150]	5.3[2.5]	7.3[3.5]	12.6[6.0]	P2	0.23[0.09]
90[110]	4.3[0.7]	6.0[1.0]	10.3[1.7]	P3	0.18[0.09]
150[160]	5.9[2.0]	8.2[2.7]	14.1[4.7]	WB	7.00[1.29]

have the dark matter in the mass range $\sim(110\text{--}190)$ GeV. This is due to the fact that the maximal energy the photon can carry is $E_\gamma^{\text{max}} = M_\chi(1 - M_W^2/M_\chi^2)$ in the process $\chi\chi \rightarrow WW\gamma$, and the energy of the monochromatic photons via $\chi\chi \rightarrow \gamma X$ is $E_\gamma = M_\chi[1 - M_X^2/(4M_\chi^2)]$. Thus the photons arising from the process $\chi\chi \rightarrow WW\gamma$ have energy whose location in the energy spectrum is at least $\sim(23\text{--}40)$ GeV below the monochromatic photons in γZ , $\gamma\gamma$ final states for dark matter mass in the range $\sim(110\text{--}190)$ GeV. For a related discussion see [36].

The Higgsino models typically have a small μ and large m_0 and lie on the boundary of the radiative electroweak symmetry breaking curve, i.e., the Hyperbolic Branch [37,38]. It is the smallness of μ relative to the soft gaugino masses that makes the three lightest particles, the two lightest neutralinos and the lighter chargino, essentially degenerate in mass [38]. In this region μ (and some of the sparticle spectrum) is very sensitive to small changes in the input parameters at the GUT scale. On the other hand, since μ is small, one is in a less fine tuned region. Alternately, instead of working down from the high scale, one could simply generate these Higgsino-like LSPs directly by inputs at the weak scale. We have checked this for the models discussed here. This is evident from Table I.

IV. POSITRONS FROM HIGGSINOS AND MIXED WINOS

Next, we discuss the positron excess prediction in the Higgsino-like model. In Higgsino and wino models, the high energy positron flux can arise from WW and ZZ production from the neutralino annihilation in the halo with approximate cross sections at leading order [16]

$$\langle\sigma v\rangle(\chi\chi \rightarrow VV) \simeq \frac{g_2^4}{C_V 2\pi M_\chi^2} \frac{(1 - x_V)^{3/2}}{(2 - x_V)^2}, \quad (2)$$

where $V = (W, Z)$, $x_V = M_V^2/M_\chi^2$, $C_W = 16(1)$ for Higgsino (wino) models and the ZZ production is only significant for Higgsino models where $C_Z = 32\cos^4(\theta_w)$. For the models (P1–P3), the LSP is mostly a Higgsino with only a very small portion being gaugino. Here the cross sections that enter in the positron excess are size $\langle\sigma v\rangle(\chi\chi \rightarrow WW, ZZ)_{\text{Higgsino}} \lesssim 4 \times 10^{-25}$ cm³/s.

The positron flux from the Higgsino dark matter can be described semianalytically (for early work, see [18]). The flux enters as a solution to the diffusion loss equation, which is solved in a region with a cylindrical boundary. The particle physics depends on $\langle\sigma v\rangle_{\text{halo}}$, and dN/dE , the fragmentation functions/energy distributions [18]. The astrophysics depends on the dark matter profile [39], and on the energy loss in the flux from the presence of magnetic fields and from scattering off galactic photons. A boost factor which parametrizes the possible local inhomogeneities of the dark matter distribution can be present. Recent results from N -body simulations indicate that large dark matter clumps within the halo are unlikely [40,41]. The boost B we consider here is small, as low as $\sim(2\text{--}3)$. The background taken is consistent with the GALPROP [42] model generated in Ref. 1 of [13]. The antiproton flux follows rather analogously (for an overview and some fits, see e.g. [43]). In this analysis the antiproton backgrounds are consistent with [44], and the results for the pure wino case considered are consistent with [6,13,15].

The full analysis is exhibited in the upper left panel of Fig. 1 where we show fits to the PAMELA positron fraction [1]. For comparison, we also show the essentially pure wino case, which requires no boost (clump), but as mentioned in the introduction, will generally lead to an overproduction of photons. Model P3 requires a boost of only $\sim(2\text{--}3)$ as the LSP is light, ~ 110 GeV. For this case, the \bar{p} flux is slightly larger at lower kinetic energy, but still consistent with the data. A pure wino at 110 GeV would give a cross section about 10 times larger relative to the Higgsino model at 110 GeV. Including the boost factor of 3 for the Higgsino model, the pure wino is then (3–4) times stronger in its flux, and this is another reason a pure wino at 110 GeV would fail—it would overproduce the antiprotons, whereas the Higgsino with minimal boost is consistent. Thus, in the upper right panel of Fig. 1 we give a comparison of the \bar{p} flux with the recently released data from Ref. 3 of [1]. Indeed, it is seen that the theoretical prediction of the \bar{p} flux is in perfectly good accord with this data. We note there are other processes beyond the leading order that could produce SM gauge boson final states. For diboson final states, these corrections are rather small and lead to a small shift downward in the clump factor used (see Ref. 2 of [45]). The minimal boost utilized here is rather different compared to those in analyses of bino-like LSPs which use boosts of size 10^2 or larger [21] to fit the data. The analysis we present does not attempt to explain the high energy $e + \bar{e}$ data [46,47]. This could be explained with an additional electron source [13].

V. SIGNATURE ANALYSIS AT THE LHC AT $\sqrt{s} = 7$ TeV

As mentioned above, some of the colored sparticles in the Higgsino-like models are rather light which is encouraging for possible early discovery of this class of models at

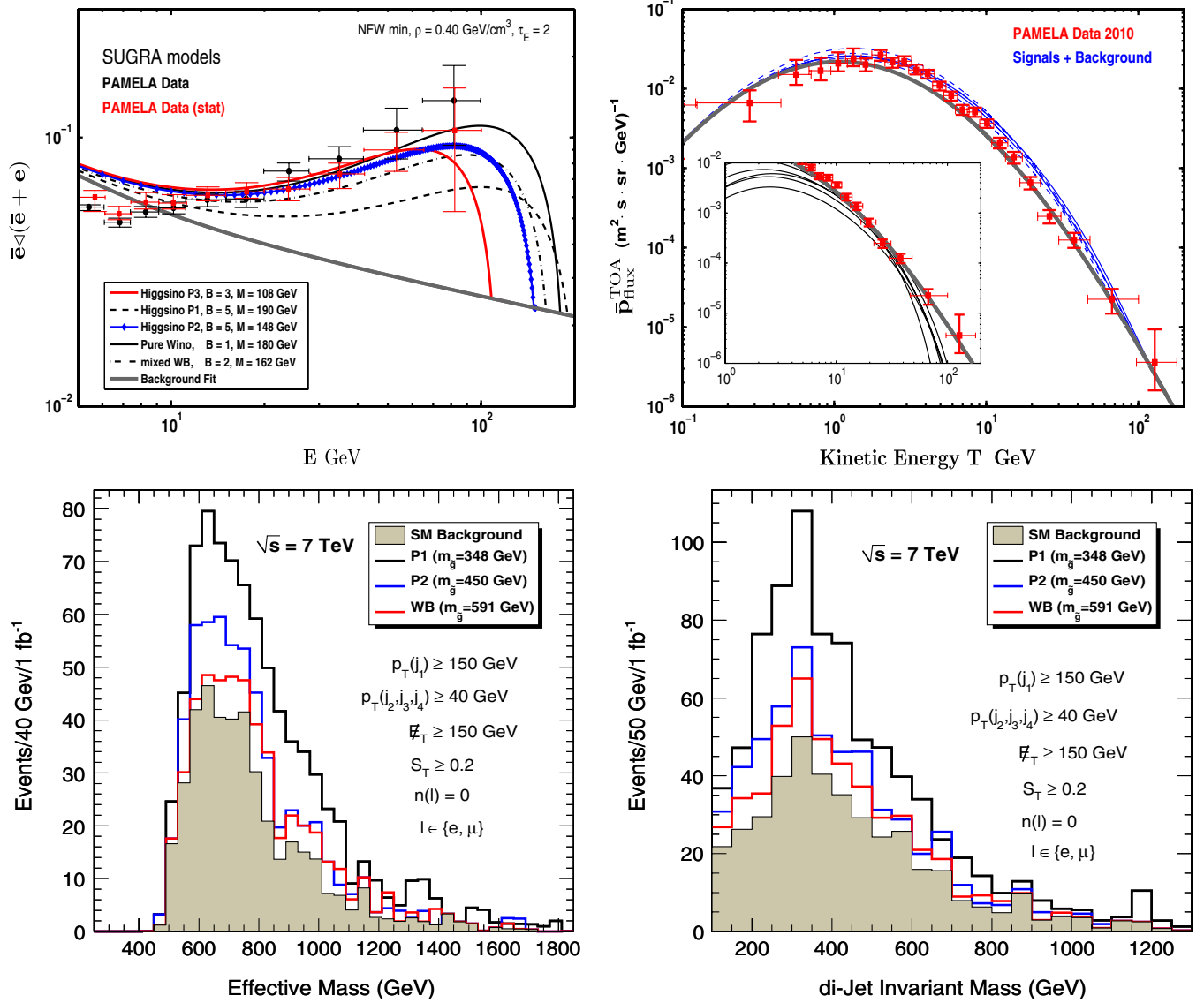


FIG. 1 (color online). Top left: PAMELA positron excess and the Higgsino models P1–P3. The wino dominated model is also shown for comparison along with a mixed wino-bino model, WB. Top right: The PAMELA \bar{p} flux and the predictions are seen to be compatible with the data. Equal dark matter densities and boosts are taken in both top panels. Lower left: SUSY background events vs effective mass at 1 fb^{-1} for the signature cuts shown in the panel for models P1, P2, and WB. Lower right: SUSY plus background events vs the di-jet invariant mass at 1 fb^{-1} for signature cuts shown in the panel for the models P1, P2, and WB. Both lower plots do not show model P3 due to its suppressed cross section at LHC-7. The legends labeling the model names (not colors) indicate the model class in all figures.

LHC-7 [48]. To achieve a significance necessary for discovery, i.e., $S \geq \max\{5\sqrt{B}, 10\}$, it is essential to have a reliable SM background computation. In our analysis we simulate the SM backgrounds [49] using MADGRAPH 4.4 [50] for parton level processes, PYTHIA 6.4 for hadronization, and PGS-4 for detector simulation [51]. The b -tagging efficiency in PGS-4 is based on the technical design reports of CMS and ATLAS [52]. The sparticle spectrum and branching ratios for the signal analysis is generated using computational packages for supersymmetric models [32].

The models we consider for the LHC-7 analysis have rather light gluinos in the mass range (~ 350 – 600) GeV. The production cross sections for these models are dominated by gluino production, and the branching fractions are dominated by either the radiative decay of the gluino $\tilde{g} \rightarrow g\tilde{\chi}_1^0$, $\tilde{g} \rightarrow g\tilde{\chi}_2^0$ (Higgsino-like model P1) or a combination of the radiative decays above and the three body decays $\tilde{g} \rightarrow \tilde{\chi}_1^\pm(b\bar{l} + \text{h.c.})$ (Higgsino-like model P2) or effectively just the 3 body decays producing both $\tilde{\chi}_1^\pm$ and $\tilde{\chi}_2^0$ with substantial rates (mixed WB model). The subsequent decays follow from the chargino and neutralino into standard

model quarks and leptons. Decays into the degenerate hidden sector particles near the LSP mass are suppressed.

In the lower left panel of Fig. 1 we give an analysis for the Higgsino models P1 and P2 with the number of SUSY events in 40 GeV bins at 1 fb^{-1} of integrated luminosity vs the effective mass defined to be the sum of the p_T of the four hardest jets plus missing energy. The cuts used are exhibited in the panel. In the lower right panel of Fig. 1 we give an analysis for the Higgsino models P1 and P2 with the number of SUSY events in 50 GeV bins at 1 fb^{-1} of integrated luminosity vs the di-jet invariant mass where the cuts used are exhibited in the panel. For comparison, we also give an analysis of the mixed WB model in both lower left and lower right panels. Since the gluino is relatively light and the squarks are heavier, the 3 body decays of the gluino dominate resulting in rich di-jet signals and effective mass. We note that while the model P3 provides a good fit to the PAMELA data and its photon flux is an order of magnitude below the current limits, it has a heavy ($\sim 1.5 \text{ TeV}$) gluino and would not produce an identifiable signal in the early LHC data.

VI. CONCLUSION

We have presented here a solution to the PAMELA data and the Fermi photon data with a Higgsino-like LSP which can also be made compliant with WMAP. It is shown that the models considered are consistent with the current very

stringent limits on $\gamma\gamma$ and γZ production from Fermi-LAT which put the pure wino LSP models close to the edge of the upper limit of experiment. Furthermore, the Higgsino LSP models are consistent with the upper limit from the XENON100 experiment and will be testable in improved dark matter experiments. We find that LHC-7 can realistically probe these models up to gluino masses of $\sim 600 \text{ GeV}$ with 1 fb^{-1} of data. However, one would need larger integrated luminosity to carry out precise mass reconstructions. The above presents an interesting possibility of having a low mass gluino from the radiative breaking of the electroweak symmetry which can be produced at the LHC in early runs and also having a mostly Higgsino LSP giving rise to PAMELA positron excess. Thus the class of models discussed here can be tested on multiple fronts.

ACKNOWLEDGMENTS

This research is supported in part by Department of Energy (DOE) Grant No. DE-FG02-95ER40899, and the U.S. National Science Foundation (NSF) Grants No. PHY-0653342, No. PHY-0704067, and No. PHY-0757959, and in addition by the NSF through TeraGrid resources provided by National Center for Supercomputing Applications (NCSA), Texas Advanced Computing Center (TACC), Purdue University, and Louisiana Optical Network Initiative (LONI) under Grant No. TG-PHY100036.

-
- [1] PAMELA Collaboration, *Nature (London)* **458**, 607 (2009); PAMELA Collaboration, *Phys. Rev. Lett.* **102**, 051101 (2009); PAMELA Collaboration, *Astropart. Phys.* **34**, 1 (2010); O. Adriani *et al.* (PAMELA Collaboration), *Phys. Rev. Lett.* **105**, 121101 (2010).
 - [2] Fermi LATPhys. *Rev. Lett.* **104**, 091302 (2010).
 - [3] D. Feldman, Z. Liu, and P. Nath, *Phys. Rev. D* **79**, 063509 (2009); M. Ibe *et al.*, *ibid.* **79**, 095009 (2009); W. Guo *et al.*, *ibid.* **79**, 055012 (2009); I. Gogoladze *et al.*, *Phys. Lett. B* **679**, 237 (2009); F. Cyr-Racine *et al.*, *Phys. Rev. D* **80**, 081302 (2009); Y. Bai *et al.*, *ibid.* **80**, 055004 (2009); X. Bi *et al.*, *Phys. Rev. D* **81**, 063522 (2010); K. Kadota *et al.*, *Phys. Rev. D* **81**, 115006 (2010).
 - [4] J. Hisano, S. Matsumoto, and M.M. Nojiri, *Phys. Rev. Lett.* **92**, 031303 (2004); M. Cirelli *et al.*, *Nucl. Phys. B* **813**, 1 (2009); N. Arkani-Hamed *et al.*, *Phys. Rev. D* **79**, 015014 (2009); M. Pospelov and A. Ritz, *Phys. Lett. B* **671**, 391 (2009); Y. Nomura and J. Thaler, *Phys. Rev. D* **79**, 075008 (2009); P.J. Fox and E. Poppitz, *ibid.* **79**, 083528 (2009).
 - [5] J.L. Feng *et al.*, *Phys. Rev. Lett.* **104**, 151301 (2010).
 - [6] D. Feldman, Z. Liu, P. Nath, and B. Nelson, *Phys. Rev. D* **80**, 075001 (2009).
 - [7] D. Feldman, Z. Liu, P. Nath, and G. Peim, *Phys. Rev. D* **81**, 095017 (2010).
 - [8] T. Cohen and K. Zurek, *Phys. Rev. Lett.* **104**, 101301 (2010).
 - [9] V. Barger *et al.*, *Phys. Lett. B* **672**, 141 (2009).
 - [10] R. Allahverdi *et al.*, *Phys. Rev. D* **79**, 075005 (2009).
 - [11] T. Moroi and L. Randall, *Nucl. Phys. B* **570**, 455 (2000).
 - [12] For review, see D. Feldman and G. Kane, *Perspectives on Supersymmetry II* (World Scientific, Singapore, 2010).
 - [13] G. Kane, R. Lu, and S. Watson, *Phys. Lett. B* **681**, 151 (2009); J. Hisano *et al.*, *Phys. Rev. D* **79**, 063514 (2009); P. Grajek *et al.*, *ibid.* **79**, 043506 (2009).
 - [14] H. Yuksel *et al.*, *Phys. Rev. Lett.* **103**, 051101 (2009); D. Hooper *et al.*, *J. Cosmol. Astropart. Phys.* **01** (2009) 025; S. Profumo, arXiv:0812.4457; P. Blasi and P.D. Serpico, *Phys. Rev. Lett.* **103**, 081103 (2009); P.L. Biermann *et al.*, *Phys. Rev. Lett.* **103**, 061101 (2009).
 - [15] D. Feldman, G. Kane, R. Lu, and B.D. Nelson, *Phys. Lett. B* **687**, 363 (2010).
 - [16] K.A. Olive and M. Srednicki, *Phys. Lett. B* **230**, 78 (1989).
 - [17] M. Drees *et al.*, *Phys. Rev. D* **56**, 276 (1997).
 - [18] E. A. Baltz and J. Edsjo, *Phys. Rev. D* **59**, 023511 (1998); L. Bergstrom *et al.*, *Astrophys. J.* **526**, 215 (1999).
 - [19] G.L. Kane *et al.*, *Phys. Rev. D* **65**, 057701 (2002); E. A. Baltz *et al.*, *ibid.* **65**, 063511 (2002); D. Hooper and J.

- Silk, *ibid.* **71**, 083503 (2005); P. Grajek *et al.*, arXiv:0807.1508.
- [20] L. Bergstrom and P. Ullio, *Nucl. Phys.* **B504**, 27 (1997); Z. Bern *et al.*, *Phys. Lett. B* **411**, 86 (1997); P. Ullio and L. Bergstrom, *Phys. Rev. D* **57**, 1962 (1998); J. Hisano *et al.*, *ibid.* **67**, 075014 (2003); F. Boudjema *et al.*, *ibid.* **72**, 055024 (2005).
- [21] L. Bergstrom *et al.*, *Phys. Rev. D* **59**, 043506 (1999); *Phys. Rev. D* **78**, 103520 (2008); R. C. Cotta *et al.*, arXiv:1007.5520.
- [22] B. Kors and P. Nath, *Phys. Lett. B* **586**, 366 (2004); *J. High Energy Phys.* 12 (2004) 005; 07 (2005) 069.
- [23] D. Feldman, Z. Liu, and P. Nath, *Phys. Rev. Lett.* **97**, 021801 (2006); *J. High Energy Phys.* 11 (2006) 007; *Phys. Rev. D* **75**, 115001 (2007).
- [24] E. C. G. Stueckelberg, *Helv. Phys. Acta* **11**, 225 (1938); V. I. Ogievetskii and I. V. Polubarinov, *JETP* **14**, 179 (1962); M. Kalb and P. Ramond, *Phys. Rev. D* **9**, 2273 (1974).
- [25] M. B. Green and J. H. Schwarz, *Phys. Lett. B* **149**, 117 (1984).
- [26] R. Blumenhagen, B. Kors, D. Lust, and S. Stieberger, *Phys. Rep.* **445**, 1 (2007).
- [27] B. Kors and P. Nath, in *PASCOS 2004: Proceedings of the 10th International Symposium on Particles, Strings, and Cosmology and Themes in Unification: The Pran Nath Festschrift* (World Scientific, Hackensack, NJ, 2005).
- [28] A. H. Chamseddine, R. Arnowitt, and P. Nath, *Phys. Rev. Lett.* **49**, 970 (1982); *Nucl. Phys.* **B227**, 121 (1983); L. Hall, J. Lykken, and S. Weinberg, *Phys. Rev. D* **27**, 2359 (1983); For a review, see P. Nath, in *International Conference BEYOND-2003, Schloss Ringberg, Germany, June, 2003* (Springer, Heidelberg, Germany, 2004).
- [29] A. Corsetti and P. Nath, *Phys. Rev. D* **64**, 125010 (2001).
- [30] D. Feldman *et al.*, *Phys. Rev. D* **75**, 023503 (2007).
- [31] WMAP Collaboration, arXiv:1001.4744.
- [32] A. Djouadi *et al.*, *Comput. Phys. Commun.* **176**, 426 (2007); B. C. Allanach, *Comput. Phys. Commun.* **143**, 305 (2002); M. Muhlleitner *et al.*, *Comput. Phys. Commun.* **168**, 46 (2005); A. Djouadi *et al.*, *Acta Phys. Pol. B* **38**, 635 (2007); G. Belanger *et al.*, *Comput. Phys. Commun.* **180**, 747 (2009).
- [33] N. Chen *et al.*, *Phys. Lett. B* **685**, 174 (2010).
- [34] XENON100 Collaboration, *Phys. Rev. Lett.* **105**, 131302 (2010); CDMS-II Collaboration, *Phys. Rev. Lett.* **102**, 011301 (2009); Z. Ahmed *et al.* (CDMS-II Collaboration), *Science* **327**, 1619 (2010).
- [35] L. Bergstrom, T. Bringmann, M. Eriksson, and M. Gustafsson, *Phys. Rev. Lett.* **95**, 241301 (2005); T. Bringmann, L. Bergstrom, and J. Edsjo, *J. High Energy Phys.* 01 (2008) 049, and references therein.
- [36] M. Cannoni *et al.*, *Phys. Rev. D* **81**, 107303 (2010).
- [37] K. L. Chan *et al.*, *Phys. Rev. D* **58**, 096004 (1998); R. L. Arnowitt and P. Nath, *Phys. Rev. D* **46**, 3981 (1992); J. L. Feng *et al.*, *Phys. Rev. Lett.* **84**, 2322 (2000); H. Baer *et al.*, *J. High Energy Phys.* 06 (2003) 054.
- [38] U. Chattopadhyay *et al.*, *Phys. Rev. D* **68**, 035005 (2003).
- [39] J. Navarro *et al.*, *Astrophys. J.* **490**, 493 (1997); B. Moore *et al.*, *Mon. Not. R. Astron. Soc.* **310**, 1147 (1999); P. Salucci and A. Burkert, *Astrophys. J.* **537**, L9 (2000).
- [40] P. Brun *et al.*, *Phys. Rev. D* **80**, 035023 (2009).
- [41] M. Kamionkowski *et al.*, *Phys. Rev. D* **81**, 043532 (2010).
- [42] I. V. Moskalenko *et al.*, *Astrophys. J.* **493**, 694 (1998).
- [43] M. Cirelli *et al.*, *Nucl. Phys.* **B800**, 204 (2008).
- [44] T. Bringmann *et al.*, *Phys. Rev. D* **75**, 083006 (2007).
- [45] M. Ciafaloni, P. Ciafaloni, and D. Comelli, *J. High Energy Phys.* 03 (2010) 072; P. Ciafaloni, D. Comelli, A. Riotto, F. Sala, A. Strumia, and A. Urbano, arXiv:1009.0224.
- [46] M. Ackermann *et al.* (Fermi-LAT Collaboration), *Phys. Rev. D* **82**, 092004 (2010).
- [47] P. Meade *et al.*, *Nucl. Phys.* **B831**, 178 (2010).
- [48] For a recent review see, P. Nath *et al.*, *Nucl. Phys. B, Proc. Suppl.* **200**, 185 (2010).
- [49] B. Altunkaynak, M. Holmes, P. Nath, B. D. Nelson, and G. Peim, *Phys. Rev. D* **82**, 115001 (2010).
- [50] J. Alwall *et al.*, *J. High Energy Phys.* 09 (2007) 028.
- [51] T. Sjostrand, S. Mrenna, and P. Z. Skands, *J. High Energy Phys.* 05 (2006) 026; J. Conway *et al.*, PGS-4, <http://www.physics.ucdavis.edu/~conway/research/software/pgs/pgs4-general.htm>.
- [52] G. L. Bayatian *et al.* (CMS Collaboration), *CMS Technical Design Report, Vol. I: Detector Performance and Software* (LHCC, Geneva, 2006); G. Aad *et al.* (ATLAS Collaboration), arXiv:0901.0512.